Ocean Science Journal (2022) 57:420–435
https://doi.org/10.1007/s12601-022-00076-w

Online ISSN 2005-7172
Print ISSN 1738-5261

ARTICLE

Multi-proxy Stratigraphy and Paleoceanographic Variations in Sediment from the Korea Plateau, East Sea (Japan Sea), Over the Last 500 kyr

Sangmin Hyun[1] · Jin-Kyung Kim[2,4] · Jeongwon Kang[2] · Gil Young Kim[3]

Received: 14 June 2021 / Revised: 8 April 2022 / Accepted: 17 April 2022 / Published online: 14 June 2022

Abstract

High-resolution geochemical measurements were performed on core E09-08, which was taken from the top flat area of the Korea Plateau in the East Sea (Japan Sea). Based on analyses of sedimentary lamination, high-resolution oxygen isotopes, alkenone sea surface temperature (SST) variations, and comparison with previous results from the eastern part of the East Sea, a detailed multi-proxy-based stratigraphy was reconstructed. The results demonstrated that the core bottom dates approximately 500 kyr in the late marine isotope stage (MIS) 13, and provides high-resolution data on the paleoceanographic regime in the study area. Biogenic components of total organic carbon (TOC), carbon and nitrogen isotopes of organic matter ($\delta^{13}C_{org}$ and $\delta^{15}N_{org}$), and alkenone concentrations indicate a paleoceanographic regime shift within the last 500 kyr. The excursion of proxies of $\delta^{18}O$, $\delta^{13}C_{org}$ and $\delta^{15}N_{org}$ and alkenone-based SST indicate two modes of oceanographic conditions: strong negative coupled mode (SNCM) during MIS 2, 10, and 12, and normal oceanographic decoupled mode (NODM) during other MIS. These two modes were interpreted as the terrestrial organic matter source domain and high-productivity oceanographic domain, respectively. The SNCM is characterized by relatively low $\delta^{13}C_{org}$ and $\delta^{15}N_{org}$, and a high C/N ratio (> 12), whereas the NODM is characterized by relatively high $\delta^{13}C_{org}$ and high $\delta^{15}N_{org}$, implying that larger amounts of terrestrial material were supplied during MIS 2, 10 and 12, with enhanced productivity during other MIS. The SNCM and NODM mode are also strongly associated with eustatic sea-level changes. The $\delta^{13}C_{org}$ and $\delta^{15}N_{org}$ values and alkenone-based SST excursions over glacial-interglacial periods were generally consistent with global-scale paleoclimate variation, as well as local paleoclimate. This study employed multi-proxy-based stratigraphy to demonstrate dramatic oceanographic variations since MIS 13, indicating that the local oceanographic setting was superimposed on global glacial-interglacial variations.

Keywords Stratigraphy · $\delta^{13}C_{org}$ and $\delta^{15}N_{org}$ · Alkenone-based SST · Paleoceanography

1 Introduction

The East Sea (Japan Sea) formed in the Early Miocene and has evolved over the past 32 myr, providing abundant geological, geophysical, and paleontological records (Burckle et al. 1992; Charvet et al. 1992; Ingle 1992). Geophysically, the structural features of the East Sea include subsidence, gravity-induced structures, large faults, and veins in the volcanic basement (Charvet et al. 1992). Sedimentologically, the East Sea is composed of typical hemipalegic sediment, with compositional variations in sediment from the late Quaternary (Tada and Iijima 1992; Tada et al. 1999; Seki et al. 2019). Due to eustatic sea-level changes and their resultant ventilation changes, laminated mud (layers) during glacial

✉ Sangmin Hyun
smhyun@kiost.ac.kr

1 Marine Environmental Research Center, Korea Institute of Ocean Science and Technology Busan 49111, Republic of Korea

2 Korean Sea Laboratory Geosystem Research Unit, Korea Institute of Ocean Science and Technology Busan 49111, Republic of Korea

3 Marine Geology and Energy Division, Korea and Institute of Geoscience and Mineral Resources Daejeon 34132, Republic of Korea

4 Present Address: Laboratory for Marine Geology, First Institute of Oceanography, Qingdao 266061, China

and bioturbated mud in interglacial periods were deposited, respectively (Bahk et al. 2000).

Several previous studies have shown that sediments below the carbonate compensation depth (CCD) are deficient in carbonate due to its dissolution. At present, the CCD of the East Sea is highly variable locally, but is located at a water depth of ca.1500 m in the San'in district of the East Sea (Ujiie and Ichikura 1973). The CCD is much shallower than this level in high-productivity coastal area near the Korea Plateau (near Dokdo Island), where it is located at around 1000 m water depth (Hyun et al. 2010; Kim et al. 2010). Therefore, sediment collected deeper than 1000 m is likely to undergo carbonate dissolution, making it difficult to collect foraminifera for oxygen isotope analysis.

Fundamental research on paleoceanographic variations in the East Sea was initiated with the first research on oxygen isotopes of foraminifera (e.g., Oba et al. 1991). This was followed by numerous studies attempting to explain the paleoceanographic and paleoclimatological variations among glacial and interglacial periods in terms of the scope of global environmental changes (Tada et al. 1999, 2018; Kim et al. 2000; Bahk et al. 2000; Hyun et al. 2007, 2013; Irino et al. 2018; Sagawa et al. 2018; Seki et al. 2019; Zhai et al. 2021). The reason for these paleoceanographic variations is that the East Sea paleoenvironment was tightly associated with dramatic changes due to the sea-level fluctuation between glacial and interglacial periods (Tada et al. 1999, 2018). Repeated high and low sea-level during interglacial and glacial periods affect the ventilation in East Sea, and then the bottom water condition has been changed into oxic and anoxic (Bahk et al. 2000, 2005). Findings related to several paleoceanographic changes are relevant here: the Younger Dryas records (Keigwin et al. 1992; Kim et al. 2000), the Dansgaard-Oeshger event (Dansgaard et al. 1993), the East Asian monsoon system (Tada et al. 1999; Yokoyama et al. 2006; Nagashima et al. 2011; Shen et al. 2017; Ao et al. 2020), regional eustatic-related paleoceanographic changes (Oba et al. 1991; Tada et al.1999, 2018; Bahk et al. 2005), and organic geochemical studies (Lee et al. 2008; Hyun et al. 2013; Kaiser et al. 2019; Wang et al. 2021; Zhai et al. 2021). These studies have all demonstrated past environmental changes within the context of global and local changes.

Most previous studies on late Quaternary paleoceanography examined the Pleistocene conditions, and reported well-defined chronostratigraphy based on lamination, oxygen isotope, and other methods (Sagawa et al. 2018; Tada et al. 2018). However, paleoceanography and its relevant stratigraphy have been restricted to marine isotope stage (MIS) 8 due to the deficiency of long piston core in Korea Plateau, East Sea (Hyun et al. 2013). Therefore, the main objective of this study was to reconstruct high-resolution multi-proxy-based stratigraphy from the Korea Plateau in the East Sea, where a topographic high is present that may reflect past oceanographic changes. We also tracked paleoceanographic environmental changes using records of carbon and nitrogen isotopes of organic matter ($\delta^{13}C_{org}$ and $\delta^{15}N_{org}$) and alkenones based on the newly defined stratigraphy of the last 500 kyr.

2 Geological Setting and Oceanography

The East Sea is one of the several semi-enclosed marginal seas in the western Pacific, and is a back-arc basin of the Eurasian continent. It is connected to the East China Sea through the Korea Strait to the south and is surrounded by the Korean peninsula, the Eurasian continent, and the Japanese islands (Charvet et al. 1992; Ingle et al. 1992). The topography of the East Sea is characterized by topographic highs in the south (Korea Plateau) and east (Yamato Rise) and small islands on the eastern side (Fig. 1a). The submarine topography is composed of three major basins: the Ulleung Basin in the south (UB), the Yamato Basin in the east (YB), and the Japan Basin in the north (JB). The Korea Plateau is located in the northern part of the Ulleung Basin. It represents a topographic high and plays a crucially important role in modulating surface and intermediate currents in the East Sea (Fig. 1a) (Ingle et al. 1992).

The deep and intermediate waters of the East Sea originate from the northern part of the shallow sea, mostly from the Russian coast due to ice melt during glacial periods (Ikehara and Itaki 2007; Yoon and Kawamura 2002). However, the surface and subsurface currents, including the Tsushima Warm Current (TWC), a branch of the Kuroshio Current (KC), flow into the southern part of the East Sea through the Korea Strait (~ 140 m water depth), and flow out to the Pacific Ocean through three shallow sills: the Soya (55 m water depth), Tsugaru (130 m water depth), and Tartar (12 m water depth) (Nitani 1972). This current pattern, however, has been restricted by bathymetric highs (sills) and glacio-eustatic sea level variations since the Quaternary (Fairbanks 1989). The studied core was taken from a plain area on the topographic high of the Korea Plateau at 1259 m water depth to obtain sediments covering a long age range, aiming to avoid the carbonate dissolution effect and any gravity-flow-related sediments, which occur frequently in continental slope areas of the East Sea (e.g., Lee et al. 1999).

The physiographical condition and related eustatic sea-level changes throughout glacial-interglacial periods are the most important factors controlling paleoceanographic variations in the study area. In particular, the lower sea level during glacial periods may have altered the current system via cessation of the surface current inflow from the south (Irino et al. 2018; Seki et al. 2019; Tada et al. 2018). As described above, such a cessation or reduction of inflow may have

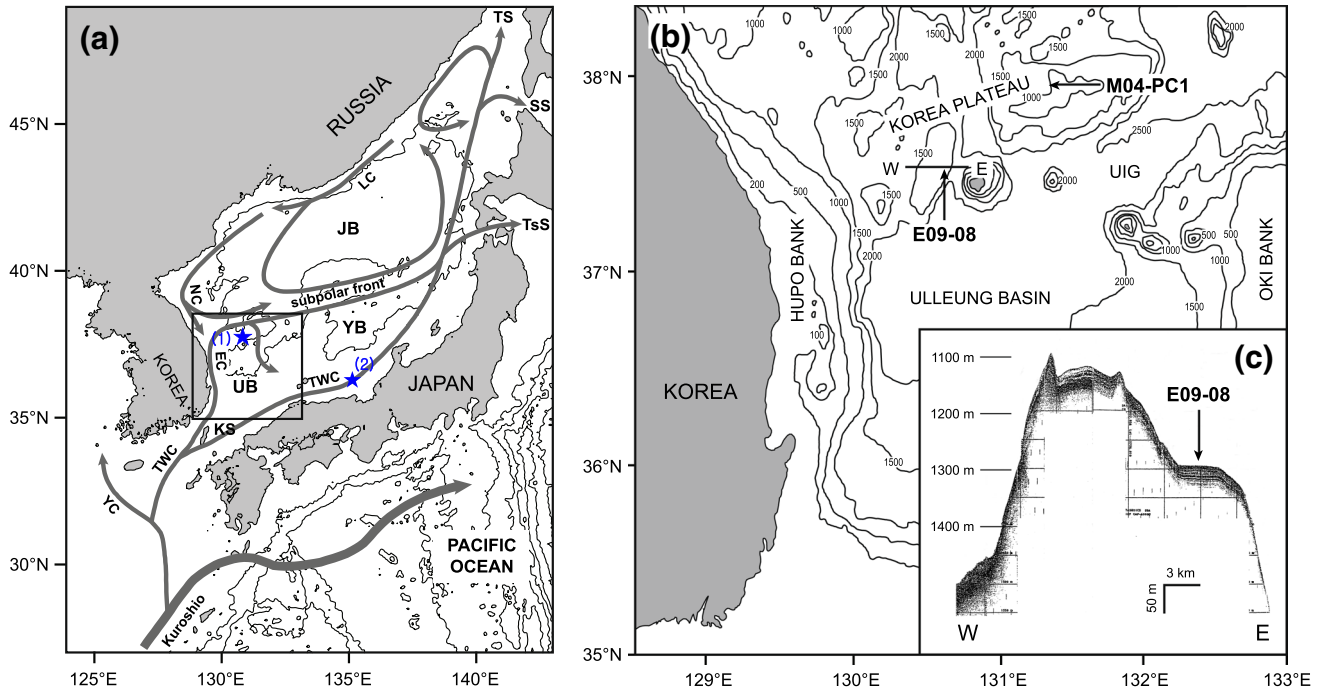

Fig. 1 **a** Surface and deep circulation patterns in the East Sea. *JB* Japan Basin; *KS* Korea Strait; *SS* Soya Strait; *TS* Tartar Strait; *TsS* Tsugaru Strait; *UB* Ulleung Basin; *YB* Yamato Basin; *EC* East Korean Warm Current; *LC* Liman Current; *NC* North Korean Cold Current; *TWC* Tsushima Warm Current; *YC* Yellow Sea Warm Current. **b** Bathymetric map of the Ulleung Basin and South Korea Plateau showing core locations and chirp track line of (**c**). **c** Chirp sub-bottom profile showing the E09-08 core location. *UIG* Ulleung Interplain Gap. Asterisks indicate sampling points. (1) This study; (2) Kido et al. (2007)

isolated the East Sea, leading to stagnant ocean circulation and likely anoxic alteration of the sedimentary environment.

3 Materials and Methods

3.1 Sample Acquisition and Description

The sediment core (E09-08) was collected from the Korea Plateau (130°36′27.48E, 37°35′40.38, 1259 m water depth) in the East Sea of Korea during the 2009 cruise of the Research Vessel *Onuri* (Fig. 1b). The core E09-08 was described under laboratory conditions after XRF scanning (*Avaatech* XRF core Scanner, Netherlands). Based on X-radiography and literatures, any changes in sedimentary structures were described to acquire basic information. High-resolution (0.1 cm interval) X-ray scanning was conducted for major and minor elements. The simplified lithological characteristics and basic information based on visual description and X-radiograph are shown in Fig. 2.

3.2 Oxygen Isotopes of Foraminifera and ^{14}C Age Dating

Planktonic foraminifera, *G. bulloides*, which are common in the East Sea, were selected for stable oxygen and carbon isotope analysis. A total of 113 samples of *G. bulloides* were reacted with dehydrated phosphoric acid (H_3PO_4)) under vacuum at 70 °C. The oxygen and carbon isotopic composition of foraminiferal samples was measured using an automated carbonate preparation device (KIEL-III) coupled to a mass spectrometer (Finnigan MAT 252) at the Environmental Isotope Laboratory in the University of Arizona. The isotopic composition measurement was calibrated based on repeated measurement of National Bureau of Standard (NBS)-19 and NBS-18 and precision were ± 0.1‰ for oxygen isotope and ± 0.08‰ for carbon isotope, respectively. The results of oxygen isotopic analyses are expressed as per mil deviation from PDB (PeeDee Belemnite) through the calibration standard. To establish a more exact core age, we also measured ^{14}C ages of planktonic foraminifera (*G. bulloides*) from four layers (26, 29, 43, and 68 cm of core depth) at the Beta Analytic, USA. Calendar ages were converted from radiocarbon ages using CALIB Rev. 6.1.1 (Stuiver and Reimer 1993). The data for the ^{14}C results,

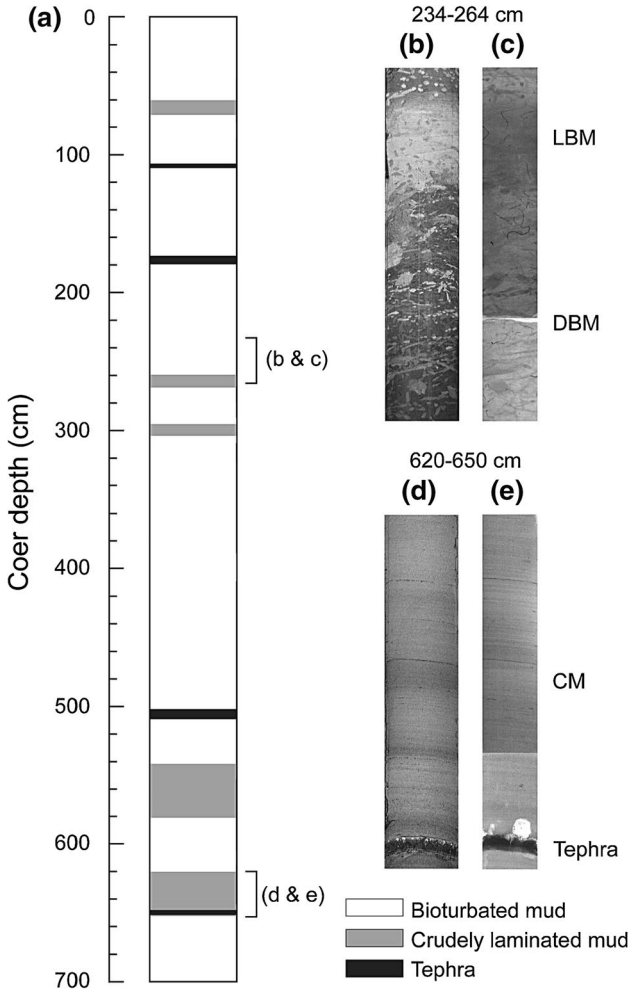

Fig. 2 **a** Simplified lithology of core E09-08. **b**, **c** Photographs of bioturbated mud facies and crudely laminated facies with tephra layer. LBM, DBM and CM indicate light bioturbated mud, dark bioturbated mud, and crudely laminated mud, respectively. **d**, **e** X-radiograph of CM and a tephra layer

foraminifer oxygen isotope, and alkenone-based SST data were combined and used to reconstruct stratigraphy.

3.3 Total Organic Carbon and Nitrogen and Their Stable Isotopes

All sediments were powdered using an agate motor and pestle after drying at 60 °C overnight. The total carbon (TC) in the powdered samples was determined by direct measurement using CHNS analyzed (EA 1112) at the Korea Institute of Ocean Science and Technology (KIOST). The total organic carbon (TOC) was determined by analyzing powdered samples treated with 1 N hydrochloric acid. The biogenic carbonate content was calculated by the difference between TC and TOC (i.e., TIC) as follows: $CaCO_3$ (wt.%) = (TC wt.%) – (TOC wt.%) × (100/12). The duplication error for the TOC and carbonate was less than 5%. Powdered samples were analyzed for carbon ($\delta^{13}C_{org}$) and nitrogen ($\delta^{15}N_{org}$) isotopes of organic matter at the Iso-Analytical Ltd., UK. The analytical errors for these $\delta^{13}C_{org}$ and $\delta^{15}N_{org}$ values were less than 5%.

3.4 Alkenones and Alkenone-Based SST

Lipids were extracted from about 5 g of dried sediment using a DIONEX Accelerated Solvent Extractor ASE-200 at 100 °C and 1000 psi for 10 min with 11 ml of (dichloromethane-methyl alcohol) CH_2Cl_2–CH_3OH (6:4) and then concentrated. The lipid extract was separated into four fractions using column chromatography (SiO_2 with 5% distilled water; I.D., 5.5 mm; length, 45 mm): F1 (hydrocarbons), 3 ml hexane; F2 (aromatic hydrocarbons), 3 ml hexane-toluene (3:1); F3 (ketones), 4 ml toluene; F4 (polar compounds), 3 ml toluene–CH_3OH (3:1); *n*-C36H74 was added as an internal standard to F3. Gas chromatography (GC) for the analysis of alkenones in F3 was conducted using a Hewlett Packard 5890 series II gas chromatograph with on-column injection and electronic pressure-control systems, and a flame ionization detector (FID). Samples were dissolved in hexane. Helium was the carrier gas and the flow velocity was maintained at 30 cm/s. A Chrompack CP-Sil5CB column was used (length, 60 m; i.d., 0.25 mm; thickness, 0.25 lm). The oven temperature was programmed to rise from 70 to 290 °C at 20 °C/min, from 290 to 310 °C at 0.5 °C/min, and to hold at 310 °C for 30 min. The standard deviations of five duplicate analyses averaged 7.5% of the concentration for each compound. All analytical procedure for alkenones concentration in Gas Chromatography (GC-6990) was referred previous works (Lee et al. 2008; Hyun et al. 2013).

Alkenones unsaturation index (UK037) was then calculated from the concentrations of di- and tri-unsaturated C37 alken-2-ones [C37MK] using the following expression (Prahl and Wakeham 1987; Prahl et al. 1988): UK37 = [C37:2MK]/([C37:2MK] + [C37:3MK]). Temperature was calculated according to the equation (Prahl and Wakeham 1987; Prahl et al. 1988): UK37 = 0.034 T + 0.039, where T = temperature [C] based on experimental results for cultured strain 55a of *Emiliania huxleyi* (Prahl et al. 1988). Analytical accuracy was 0.24 °C in the laboratory.

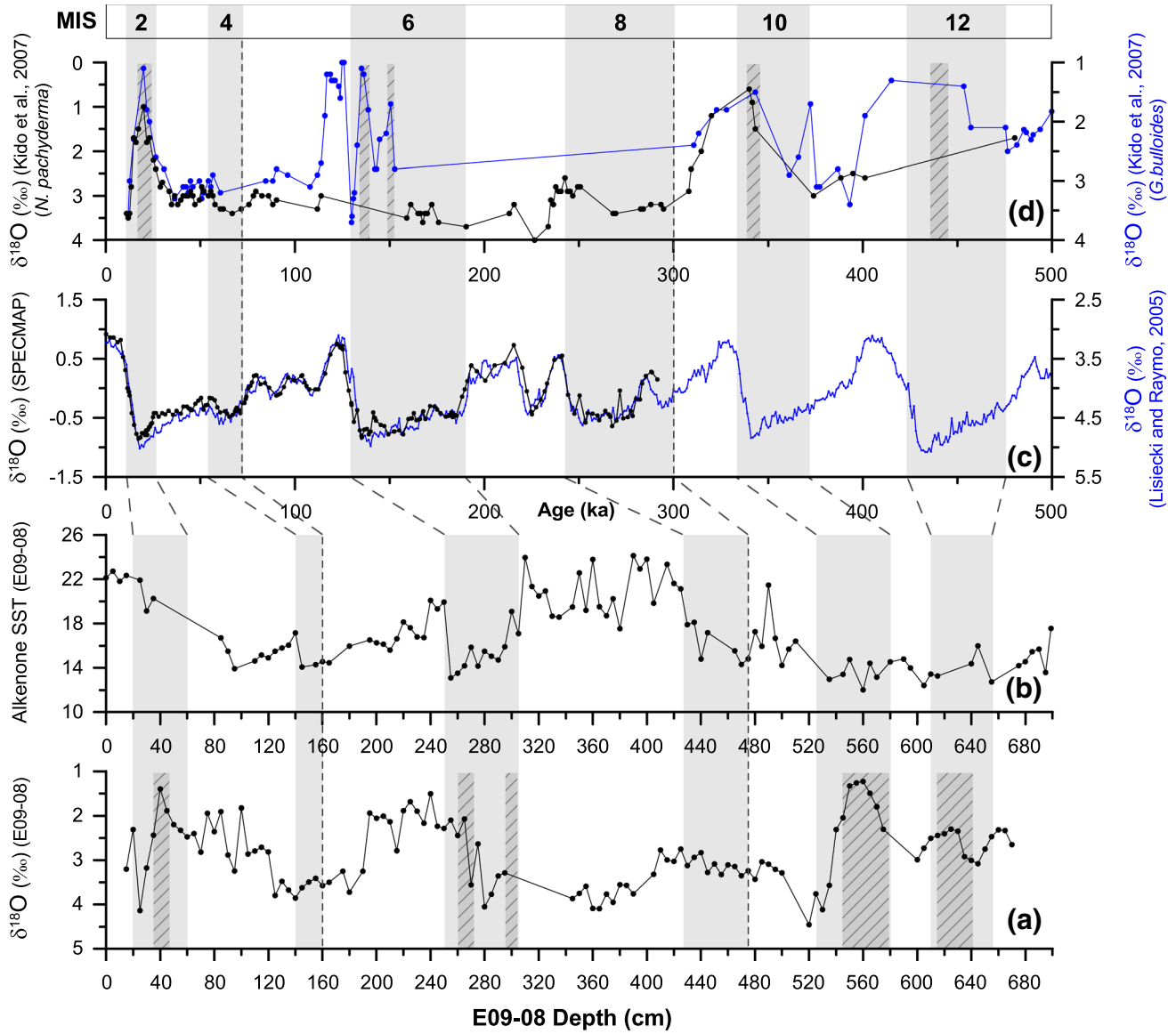

Fig. 3 **a** Profiles of $\delta^{18}O$ variations from planktonic foraminifera and sediment lamination in core E09-08, **b** Alkenone-based sea-surface temperature (SSTs) in core E09-08, **c** Spectral Mapping Project (SPECMAP; Martinson et al. 1987) for stratigraphic establishment, which revealed that the age of the bottom reached 500 kyr, at the end of Marin Isotope Stage (MIS) 13. **d** Profiles of $\delta^{18}O$ variations from two planktonic foraminifera species and laminated layers in core MD01-2407 (Kido et al. 2007)

4 Results

4.1 Oxygen Isotope ($\delta.^{18}O$)

A total of 112 *G. bulloides* samples were analyzed; their $\delta^{18}O$ fluctuations are shown in Fig. 3a. The maximum (4.5 ‰) and minimum (1.23‰) (ave. = 2.9, SD = 0.74) values occurred at core depths of 520 cm and 560 cm, respectively. Overall, $\delta^{18}O$ excursion showed high fluctuation throughout the depth, with lower values in laminated layers indicating glacial periods. These depleted values correspond to similarly low values reported in previous work (Kido et al. 2007), as shown in Fig. 3d.

4.2 Alkenone Concentration and Alkenone-Based SST

The concentrations of total C_{37} alkenones ($C_{37:2} + C_{37:3} + C_{37:4}$) exhibited strong fluctuations throughout the core (Fig. 6) with a range of ca. ~ 1840 *ug*/g ($n = 102$, ave. = 179, SD = 287) and a time-dependent trend (Figs. 3 and 6). Higher $C_{37:4}$ alkenone concentrations were found during glacial periods, but they fluctuated widely between

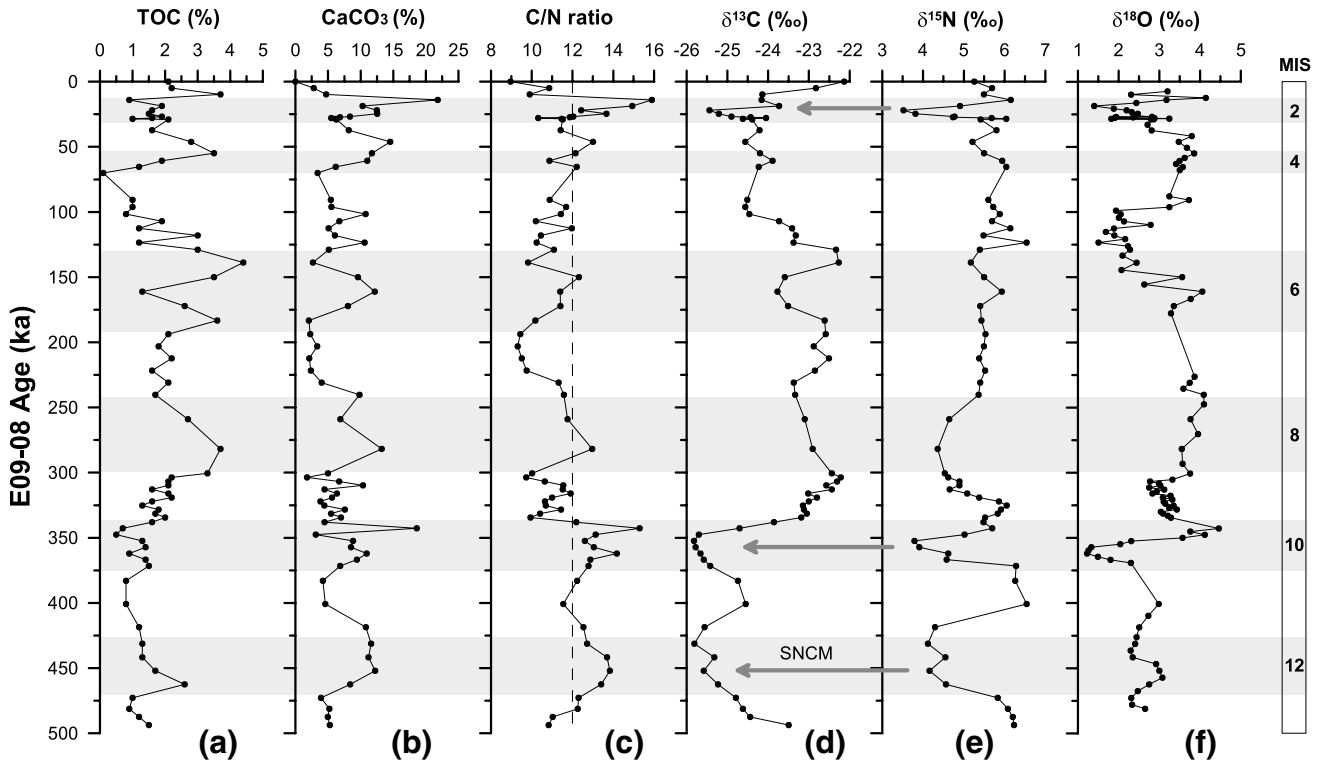

Fig. 4 Time-dependent variations in total organic carbon (TOC, %), CaCO3 (%), the carbon/nitrogen (C/N) ratio, and $\delta^{13}C_{org}$ and $\delta^{15}N_{org}$ ratios of organic matter with oxygen isotope of foraminifera ($\delta^{18}O$) from the core. Both $\delta^{13}C_{org}$ and $\delta^{15}N_{org}$ ratios can be divided into two categories: strong negative coupled mode (SNCM) and normal oceanographic decoupled mode (NODM). Arrows indicate SNCM, and shown MISs 2, 10, and 12 only

glacial and interglacial periods. SSTs calculated based on UK_{37} ranged from 12.0 to 24.1 °C and fluctuated widely between glacial and interglacial periods. Notably, the UK_{37}-based SST at MIS 8 was not as low as those of other glacial MISs (Fig. 6).

4.3 TOC and $\delta^{13}C_{org}$ and $\delta.^{15}N_{org}$

TOC content ranged from 0.1 to 4.4% (average, 1.8%, SD = 0.9, $n = 69$) and the carbonate content ranged from 1.8 to 21.8% (average, 7.4%, SD = 4.0, $n = 68$) in the studied core. The time-dependent profiles of $\delta^{13}C_{org}$ and $\delta^{15}N_{org}$ for core E09-08 are shown in Fig. 4, with $\delta^{13}C_{org}$ ranging from − 25.8 to − 22.1‰ (average, − 23.9‰, SD = 1.1, $n = 69$) and $\delta^{15}N_{org}$ showed moderate variation, ranging from 3.5 to 6.5‰.

5 Discussions

5.1 Multi-proxy Stratigraphy

5.1.1 Sedimentary Structure and Glacial Records of Laminated Mud

Based on X-radiography and the literatures, several distinctive sedimentary structures were observed in the studied sediment core (Fig. 2). As reported in several previous studies, core sediments showed typical hemipelagic characteristics and contain biogenic materials such as organic carbon and $CaCO_3$, as well as terrestrial organic matter and aeolian dust driven by strong winds, thereby reflecting surrounding environmental changes (Bahk et al. 2000; Irino and Tada 2002; Yokoyama et al. 2006; Nagashima et al. 2011; Hyun et al. 2013). Lithological changes are strong indicators of various oceanographic and environmental changes.

The outstanding feature of the studied core is the occurrence of thin and thick laminated layers, which can be used to establish a reliable stratigraphy. As described previously, large amounts of freshwater could be transported from neighboring regions during glacial periods, leading to water-column stratification, a stagnant ocean, and anoxic bottom

conditions (Oba et al. 1991; Lee and Nam 2003). Weak ventilation and freshening of the surface water promote anoxic bottom conditions, causing thin or thick laminated layers to form, as shown in Fig. 2 (Tada et al. 1999, 2018; Bahk et al. 2000; Watanabe et al. 2007). As a sedimentological feature, this alternating dark/light lamination series indicates alternating sedimentary environmental changes and provides an important tool for stratigraphic comparison, supporting the establishment of a reliable chronostratigraphy (Tada et al. 1999; Bahk et al. 2000; Khim et al. 2008; Hyun et al. 2013; Tada et al. 2018). This distinctive lamination pattern that formed during the glacial period in East Sea makes it possible to correlate the lithological units at a basin-wide scale (Khim et al. 2009; Irino et al. 2018).

Such laminations were observed at several depths in our sediment column (Fig. 2). As noted above, the East Sea has experienced lowered sea level during glacial periods, and laminations usually occurs in glacial sediment. Based on detailed observations of X-radiographs, lamination was identified at five depth intervals in this study. In other words, the formation of this lamination was favored under conditions of weak ventilation and anoxic and/or dysoxic bottom water during glacial periods. Therefore, every depth at which lamination occurred can be defined as sediment deposited during a glacial period. However, laminations did not occur in all glacial sediment layers; therefore, lamination formation may have been associated with multiple factors such as water depth and the degree of ventilation.

A previous study conducted at the other side of the East Sea also examined five distinctive lamination layers over the past 640 kyr (Kido et al. 2007) and reported that the occurrence of lamination accompanied orbital-scale variations (Fig. 3). These basin-wide laminations were observed in the present study during MIS 2, 6, 10, and 12; however, no lamination was present during MIS 8. Therefore, MIS 8 did not undergo the same oceanographic ventilation and bottom conditions. Assuming that lamination is likely to occur under the conditions of slow ventilation and anoxic bottom water, paleoceanographic conditions of the bottom water may not have been sufficiently anoxic during MIS 8. Thus, water exchange with open ocean was very limited during MIS 2, 6, and 10. The sediment characteristics in combination with heavier oxygen isotope ratio and higher alkenone concentrations observed during MIS 8 may indicate dysoxic ocean conditions.

5.1.2 Oxygen Isotope Stratigraphy

Generally, the $\delta^{18}O$ of planktonic foraminifera is a powerful tool for the establishing stratigraphy of marine sediment cores as well as tracking of oceanographic variations. As isotopic signals show synchronized fluctuations over the whole world and at all ocean depths, they have been used for chronological comparisons of marine sediments (e.g., Martinson et al. 1987; Lisiecki and Raymo. 2005). In the same way, the oxygen isotopes of foraminifera have been analyzed to evaluate paleoceanographic evolution in the East Sea, showing that numerous oxygen isotope fluctuations reflect past global paleoclimate and paleoceanographic variations during the Quaternary (Oba et al. 1991; Kim et al. 2000; Kido et al. 2007). However, the oxygen isotope signal is not continuous in some sediment deposited below the CCD, and it is therefore necessary to conduct multi-species analyses or compensate for the missing values using other proxies.

At the Spectral Mapping Project (SPECMAP) scale, isotope variations clearly show a decreasing trend during interglacial periods and higher values during glacial periods. The oxygen isotope results exhibit large fluctuations throughout, with a difference of about 3‰ between higher and lower values, as shown in Fig. 3. The oxygen isotope results of the core examined in this study do not follow the global SPECMAP trend, but instead show opposite trend during the glacial periods of MIS 2 and 6, as well as potentially MISs 10 and 12. The appearance of negative peaks of this oxygen isotope during glacial periods is an important characteristic of the East Sea sediment, as demonstrated in previous studies (Kido et al. 2007; Sagawa et al. 2018). Negative peaks of $\delta^{18}O$ are caused by surface water freshening at euastatic sea levels lower than 120 m (Oba et al. 1991; Ikehara and Itaki 2007; Kido et al. 2007; Sagawa et al. 2018).

Thus, except for low values during MIS 2, 6, 10 and 12, our oxygen isotope excursion followed SPECMAP pattern, reflecting fairly good high-resolution oxygen isotope records over the last 500 kyr (Fig. 3a). As noted previously, this

Table 1 Age control points for core E09-08

Depth (cm)	Methods/Markers	Calendar Age (ka)
26	^{14}C/*G. bulloides*	12.8
29	^{14}C/*G. bulloides*	13.9
43	^{14}C/*G. bulloides*	20.1
68	^{14}C/*G. bulloides*	26.7
102–111	AT (ash)	29.4
160	Alkenone-SST	71.6
170–175	Aso-4	88
250	Alkenone-SST	129.8
305	Alkenone-SST	190.3
428	Alkenone-SST	242.7
475	Alkenone-SST	299.4
525	Alkenone-SST	334
580	Alkenone-SST	371.7
610	Alkenone-SST	422.6
655	Alkenone-SST	475.4
700	Alkenone-SST	500

freshwater influx causes a relatively high-intensity negative shift in oxygen isotope values, which was observed at the last glacial maximum (LGM) and has been employed as a stratigraphic criterion (Oba et al. 1991; Kim et al. 2000; Kido et al. 2007). We argue that the difference in oxygen isotope values between core E09-08 and SPECMAP arises from the freshwater inputs and subsequent anoxic conditions in the East Sea during glacial periods.

In terms of the radiocarbon isotope age span, supplementary ^{14}C age data and several tephra layers were analyzed to enhance the accuracy of the chronology (Table 1). The upper two ^{14}C ages samples (26 cm and 29 cm) correspond to 12.7 ka and 13.8 ka, during the transitional period from the LGM to the Holocene. The lower two ^{14}C ages also belong to glacial periods of MIS 2, and their relatively low oxygen isotope values reflect freshwater input during the glacial period. Similar isotopic decrease occurred MIS 6, 10 and 12. Therefore, decreasing trends of these oxygen isotope excursions were in the opposite direction of the trends in SPECMAP. In conclusion, the high-resolution oxygen isotope stratigraphy of core E09-08 revealed detailed records reaching back over 500 kyr. This refined geochemical chronostratigraphy enables tracking of high-resolution paleoceanographic variations in the East Sea around the Korea Plateau.

5.1.3 Alkenone Sea Surface Temperature (SST)-Based Stratigraphy

In addition to the oxygen isotope of foraminifera, sedimentary organic alkenones represent a powerful tool for reconstructing stratigraphy and oceanographic conditions (Brassell et al. 1986; Prahl and Wakeham 1987; Sawada and Handa 1998; Ishiwatari et al. 1999). As alkenones are refractory compounds even in sediment deposited below the CCD, it has been used for stratigraphic comparisons of the sediment cores with poor yields of planktonic foraminiferal tests (e.g., Brassell et al. 1986; Hyun et al. 2013).

In this study, alkenone-based SST changes show larger fluctuations, ranging between about 23 °C and 14 °C, and follow the pattern of global oxygen isotope excursions from MIS 1 to 9, compared with the SPCEMAP curve (Fig. 3). In particular, comparison between the alkenone-based SST variations and SPECMAP data shows a strong resemblance through MIS 5 to 9. However, alkenone-based SSTs show relatively high values in MIS 2, which is not synchronous with $\delta^{18}O$ trend of foraminifera. Higher SSTs during MIS 2 have been reported in previous studies (Oba et al. 1991; Ishiwatari et al. 1999; Hyun et al. 2013). In addition, the excursions of alkenone-based SST do not follow those of isotope excursions during MIS 10–12.

The important characteristic of the excursions in alkenone-based SST is the low SST at the end of MIS 6, and the very similar low SST range with minor variation during MIS 10–12. As this particular excursion differs from the alkenone-based SST stratigraphy by Brassell et al. (1986), our alkenone-based SST excursion during MIS 6 and MIS 10–12 may reflect local phenomenon. Another major characteristic of the alkenone-based SSTs used in this study is the extremely high SSTs during MIS 2, when the freshwater effect occurred and sea level was low (Oba et al. 1991; Ishiwatari et al. 1999; Hyun et al. 2013). This specific excursion has been noted in previous studies, and the present isotopic results indicate extremely high SSTs during the LGM.

In previous work of Hyun et al. (2013), the alkenone-based SST during the end of MIS 6 and 8 reached ~ 8 °C at the eastern part of the Korea Plateau, slightly lower than in this study. However, SST during MIS 10–12 has not been reported to date at the Korean Plateau. These small changes in SST during MIS 10–12 are considered a specific oceanographic characteristic of the studied area, and may be associated with local oceanographic changes such as severe cold condition with relatively shallow water depth and very weak ventilation. However, excluding the laminations, which likely formed during a glacial period with weak ventilation and dysoxic bottom conditions, this interval clearly shows low SST, with two distinctive laminations corresponding to MIS 10 and MIS 12, as shown in Fig. 3. The deficiency of oxygen isotope signals was overcome with the use of alkenone-based SST, resulting in robust alkenone-based stratigraphy for the last 500 kyr.

Alkenone $C_{37:4}$ can provide much information about paleosalinity (Harada et al. 2008; Kaiser et al. 2019; Wang et al. 2021). As shown in Fig. 6, the percentage of $C_{37:4}$ fluctuated greatly, with sharp increases during glacial periods. Because this compound can be an indicator of surface-water freshening, we attribute increased $C_{37:4}$ content during glacial periods to surface water freshening. Therefore, high $C_{37:4}$ content of implies that the estimated alkenone-based SSTs may not reflect real SSTs during MIS 10–12.

5.2 Excursions of Biogenic Components

5.2.1 TOC and Carbonate Content

Organic carbon and biogenic carbonate are crucial components of the biogenic fraction in hemipelagic sediments because they are strongly related to the global carbon cycle through biogenic productivity over long geological timescales. Numerous previous researchers have shown that TOC and carbonate modulate atmospheric carbon dioxide concentrations and the fluctuation of CCD in the ocean (e.g., Farrell and Prell 1989; Feely et al. 2008). In this context, several studies have demonstrated high fluctuations in TOC and carbonate contents in the East Sea. In particular, the carbonate content showed extreme fluctuations from near 0 to ~ 40% (e.g., Hyun et al. 2007; Suh et al. 2013). This strong

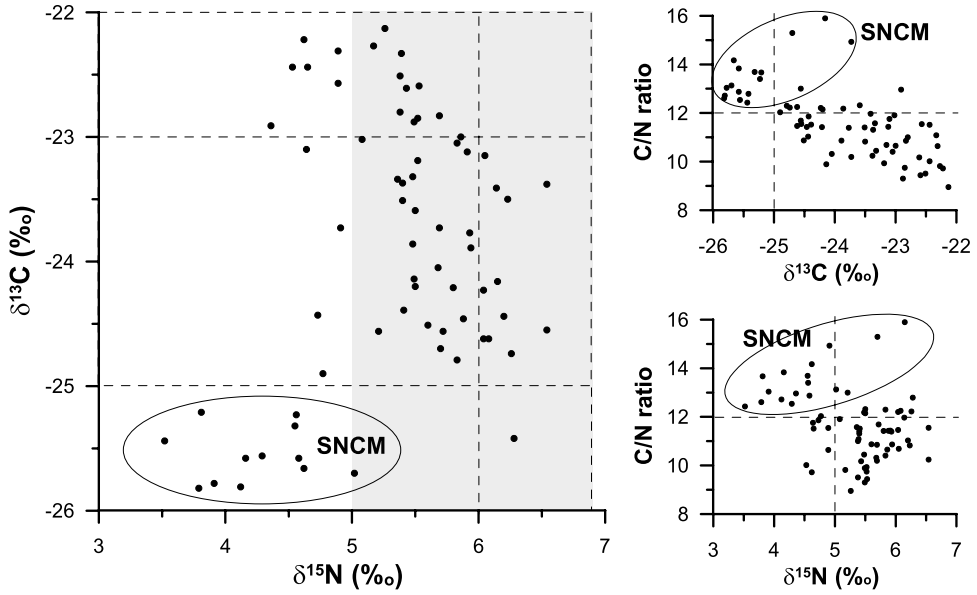

Fig. 5 Relationship between $\delta^{13}C_{org}$ and $\delta^{15}N_{org}$ in E09-08 (**a**), Relationship between C/N ratio and (**b**) $\delta^{13}C_{org}$ values and (**c**) $\delta^{15}N_{org}$ values. Strong negative coupled mode (SNCM) is indicated by circles

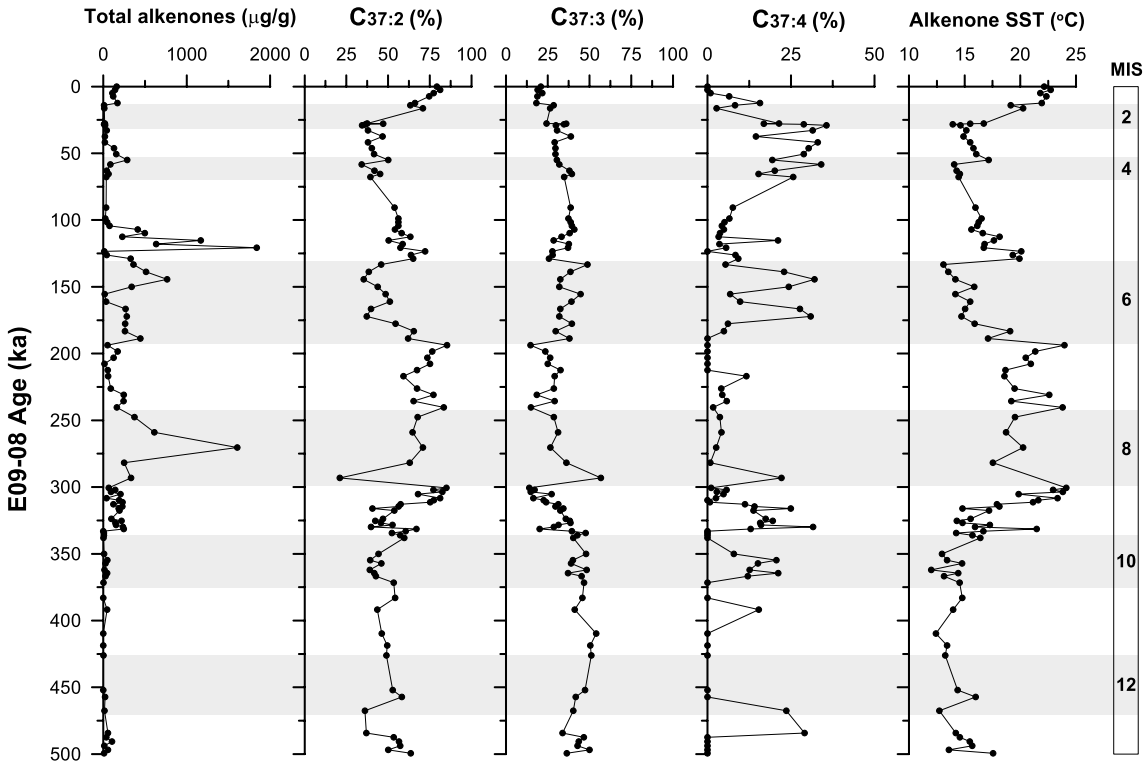

Fig. 6 Vertical profiles of total alkenones concentrations and the relative proportions of $C_{37:2}$ (%), $C_{37:3}$ (%) and $C_{37:4}$ (%). $C_{37:4}$ (%) increased during glacial periods (shaded), and alkenone-based SST variation and MISs are shown

fluctuation of carbonate content has been interpreted as a consequence of CCD changes (Ujiie and Ichikawa 1973).

As shown in Fig. 4, TOC generally did not show any distinctive trends associated with glacial and interglacial periods; TOC content was slightly higher during MISs 6, 8, and 12. The carbonate content of the core clearly increased during glacial periods and decreased during interglacial periods. In previous research, the carbonate content during glacial periods was found to be as much as four to five times higher than that in the Holocene in the Ulleung Basin core sediments, indicating that carbonate and opal content represent two alternating components in the East Sea (Hyun

et al. 2007; Khim et al. 2008). The fluctuation in carbonate content in the current study, therefore coincides with the previous research; the carbonate content has been found to be predominantly biogenic during the glacial period (Hyun et al. 2007; Suh et al. 2013).

Both TOC content and C/N ratio have been used to determine sedimentary environmental changes and organic matter sources (Stein 1990; Lamb et al. 2006). Usually, the C/N ratio of organic matter with terrestrial origins is greater than 12, and when the value is less than 12 the source is considered to be marine (Tyson 1995; Lamb et al. 2006). In the present study, higher C/N ratios (> 12) were observed at MIS 2, 10, and 12, indicating that high levels of terrestrial organic carbon were supplied from land. Although high C/N ratios are not always associated with the terrestrial source (e.g., Nakatsuka et al. 1995), the C/N ratios in this study imply that a large portion of the preserved organic material was transported from neighboring areas. However, even if the input of terrestrial organic matter during these periods was high, the TOC content was not higher than in other intervals (Fig. 4). This finding demonstrates that a high TOC content alone does not indicate enhanced productivity.

The increase in carbonate content coincided with the higher C/N ratio (> 12) (Fig. 4). The elevated carbonate content during the glacial period may have been associated with carbonate dissolution, carbonate production and/or dilution by terrestrial materials (Stein 1990). The mechanism responsible for this variation in carbonate content is beyond the scope of this study; however, terrestrial carbonate materials may have been supplied from dry continental area to the East Sea during glacial periods (Oba and Pedersen 1999), leading to high levels of terrestrial carbonate being preserved in core sediments in the East Sea.

5.2.2 Excursions $\delta^{13}C_{org}$ and $\delta.^{15}N_{org}$

$\delta^{13}C_{org}$ (‰) ratios in sedimentary organic matter are controlled by various factors including organic matter sources, degradation and/or diagenetic alternation of organic matter after deposition, and productivity changes (Altabet and Francois 1994; Nakatsuka et al. 1992, 1995; Freudenthal et al. 2001; Lehnamnet al. 2002; Naidu et al. 2000; Nagel et al. 2009; Mobius et al. 2011). Thus, $\delta^{13}C_{org}$ values are influenced by variation phytoplankton growth rates and terrestrial carbon contribution (Naidu et al. 2000), and $\delta^{13}C_{org}$ variation in sediment cores can provide diverse information. Similarly, $\delta^{15}N_{org}$ (‰) is strongly associated with nitrogen in surface water and with diagenetic alteration. In particular, $\delta^{15}N_{org}$ appears to be useful for tracking environmental changes in the East Sea, as the ocean conditions switched between anoxic and oxic environments during the glacial and interglacial periods (Oba et al. 1991; Bahk et al. 2000). Generally, marine plankton sources have heavier isotopes, whereas higher plant sources have lower isotopes. Specifically, low values of $\delta^{13}C_{org}$ (ca. -27‰) indicate a terrigenous C_3 plant source (Lim and Fujiki 2011).

Overall, both $\delta^{13}C_{org}$ and $\delta^{15}N_{org}$ ratios fluctuated in a synchronous manner. The entire area can be divided into two domains according to $\delta^{13}C_{org}$ and $\delta^{15}N_{org}$ values, and C/N ratio. In this study, simultaneous decrease in both $\delta^{13}C_{org}$ and $\delta^{15}N_{org}$ values with increased C/N ratio were observed during MIS 2, 10 and 12. Therefore, we regard this specific excursion as a strong negative coupled mode (SNCM) during MIS 2, 10 and 12 and others are normal oceanographic decoupled mode (NODM) during all other periods (Figs. 4 and 5). Notably, SNCM conditions were observed only in the glacial periods of MIS 2, 10 and 12, whereas no similar trend was observed in MIS 6 and 8. Therefore, the excursions $\delta^{13}C_{org}$ and $\delta^{15}N_{org}$ values differed among glacial periods, and appear to have depended on local productivity or the supply of terrigenous organic materials.

Previously, Khim et al. (2008) noted extraordinarily co-varying $\delta^{13}C_{org}$ and $\delta^{15}N_{org}$ values (lower shift of $\delta^{13}C_{org}$ and $\delta^{15}N_{org}$) in sedimentary organic matter collected from four sediment cores from the Japan Basin, Yamato Basin, and Korea Plateau in the East Sea. These co-varying $\delta^{13}C_{org}$ and $\delta^{15}N_{org}$ signals occurred particularly in thick and dark laminated mud layers in MIS 2 and MIS 6 in the main basin of the East Sea. They were interpreted as a consequence of the enhanced contribution of terrestrial organic detritus and anoxic diagenetic conditions in the bottom water during these times. Thus, simultaneous decrease in both $\delta^{13}C_{org}$ and $\delta^{15}N_{org}$ values are attributable mainly to terrestrial input and minor denitrification due to the bacterial activities under anoxic conditions.

In some restricted environments, diagenetically processed material can have affected on $\delta^{15}N_{org}$ values. Huge differences in $\delta^{15}N_{org}$ values have been found between the interglacial and glacial periods (Ganeshram et al. 2000). Under certain condition, denitrification after deposition was the most influential factor. Denitrification can occur in oxygen-deficient bottom environments. Bacterial activity preferentially removes ^{14} N nitrate, resulting in ^{15} N enrichment during denitrification. Denitrification records in sediment deposited during glacial and interglacial periods have revealed a difference of ca. 3‰ (Emmer and Thunell 2000; Ganeshram et al. 2000). A previous study showed that nitrogen isotope values decreased to ~ 3‰ below initial values under anoxic conditions, whereas these values increased by 3‰ under oxic conditions (Emmer and Thunell 2000).

In our study, low $\delta^{13}C_{org}$ occurred in MIS 2, 10, and 12, reflecting contributions from terrestrial sources. However, these shifts toward lighter values did not always occur during glacial periods (Fig. 4). Additionally, $\delta^{13}C_{org}$ and $\delta^{15}N_{org}$ ratios were strongly associated with marine productivity.

Thus, high productivity increased the $\delta^{13}C_{org}$ values in the sediment. Therefore, the higher trends occurring in MIS 6, 7, 8 and 9 in the examined core may reflect high productivity (Fig. 5). Higher TOC contents and moderate carbonate contents were also observed, and the C/N ratio of this interval remained below 12, indicating increased oceanic productivity.

In the present study, strong negative anomalies were observed during the MIS 2, 10, and 12 glacial periods, and differences in $\delta^{15}N_{org}$ values of ~ 3‰ were observed between glacial and interglacial periods in core E09-08 (Fig. 4). Similar to the variation in $\delta^{13}C_{org}$, that in $\delta^{15}N_{org}$ did not vary significantly between MIS 5 to MIS 9. As noted above, the behavior of $\delta^{15}N_{org}$ is strongly associated with nitrate utilization in the corresponding surface water. Therefore, this interval of high $\delta^{15}N_{org}$ with low variation may be attributable to active surface-water circulation and high productivity as supported by the finding that high-productivity area generally showed high δ^{15} N content in Pacific margin sediments over the past 120 kyr (Calvert et al. 1992; Kienast et al. 2002).

The 3‰ difference between glacial and interglacial cannot be explained by glacial–interglacial differences alone, as the $\delta^{15}N_{org}$ differences in the current study were ca. 3–4‰. Given that the samples examined in this study involved several laminated layers and low $\delta^{15}N_{org}$ values, different ocean conditions may have prevailed after MIS 13, and denitrification during MIS 2, 10 and 12 cannot completely be excluded. The ocean conditions appear to have been non-uniform in terms of $\delta^{13}C_{org}$ and $\delta^{15}N_{org}$ excursions, suggesting that some of the factors controlling $\delta^{13}C_{org}$ and $\delta^{15}N_{org}$ values have changed since MIS 13. As previously mentioned, the laminated sediment layers had the most distinctive characteristics of all depositional features in the East Sea.

Despite some consistency between the $\delta^{13}C_{org}$ and $\delta^{15}N_{org}$ values and the occurrence of laminated layers, the $\delta^{13}C_{org}$ and $\delta^{15}N_{org}$ excursions indicate strong association with both sedimentary and bottom condition. In a neighboring core (M04-PC1A), lamination was absent in MIS 2, unlike at other sites (Hyun et al. 2013). Thus, the sedimentary environment of the studied area differed from other sites, as shown by the excursion of $\delta^{13}C_{org}$ and $\delta^{15}N_{org}$, which differ from those of other sites. The shallow depth of the core site analyzed in this study may have caused these differences, as thick lamination is prevented by shallow depth and occasional active circulation.

Alternating periods of SNCM and NODM occurred over the past 500 kyr. SNCM was observed only during MIS 2, 10, 12, whereas during other MISs NODM occurred. Therefore, these two modes are not consistent with the glacial-interglacial pattern; rather, NODM occurred in MIS 9 to MIS 5, which include both glacial and interglacial periods. Specifically, some small variations in C/N ratio, and $\delta^{13}C$ and δ^{15} N values are apparent even though the alkenone-based SSTs follow a typical glacial and interglacial mode during this interval. Therefore, the occurrence of NODM between MIS 9 and MIS 5 can be regarded as representing transitional periods, which might have been influenced by local oceanographic variations such as productivity and active circulation rather than the global glacial-interglacial cycle.

Tada et al. (1999) demonstrated that paleoceanographic and paleoclimatic variations in the East Sea are strongly associated with glacio-eustatic sea level changes, and the resulting sedimentolgical characteristic have been linked to humid conditions in eastern Asia. In particular, the fluctuations between high and low TOC contents and thinly laminated layers are caused by the four modes arising from changes in sea level. In the present study, only two of these oceanographic modes are dominant, and thus, the four-mode classification used in major basin is not appropriate for the Korea Plateau.

5.2.3 Alkenone Concentration and Alkenone-Based SSTs

Total C_{37} alkenone concentrations ($C_{37:2} + C_{37:3} + C_{37:4}$) exhibit strong fluctuations throughout both glacial and interglacial periods (Fig. 6). The total concentrations of C_{37} alkenones in this study are much lower than corresponding values from the Bering Sea (Harada et al. 2003) and are very similar to those from the Sea of Okhotsk (Harada et al. 2008). The C_{37} concentrations in this study are also similar to the values reported by Lee (2007) from the Ulleung Basin in the East Sea, and by Hyun et al. (2013) from a sediment core (M04-PC1A) collected in the eastern part of the Korea Plateau in the East Sea. These similarities imply that the total C_{37} alkenone concentrations acquired here are reasonable and can be considered as an indicator of paleoceanographic variations. However, the total C_{37} alkenone concentrations show a wide range of fluctuations, with very low concentrations during MIS 2, 10, and 12. In particular, $C_{37:4}$ concentrations, which are considered as an index of salinity than SSTs or paleo-SSTs in shallow ocean environments (Bendel et al. 2005; Harada et al. 2003; Wang et al. 2021), were higher during MIS 2–4, 6, 8–10, probably associated with an enhanced freshwater supply during those periods (Fig. 6).

The alkenone-based SST variations observed in this study were characterized by lower SSTs during MIS 6, 8, 10, and 12 then during MIS 5, 7, and 9. The mean alkenone-based SST was lowest (~ 14 °C) at the end of MIS 6, and was generally higher during MIS 7. The similarity between the SST excursions and the SPECMAP oxygen isotope values indicates that the SST variations may reflect glacial and interglacial climatic changes between MIS 9 and MIS 1. However, SSTs did not reflect glacial condition during MISs 10 and

12 (Fig. 3). This implies that the oceanic conditions might have been different for these glacial periods than for other glacial periods, since alkenone-based SST can be influenced by changes in the haptophytes community between ocean-dwelling and brackish species (Kaiser et al. 2019). It should be noted that several previous studies have suggested that $C_{37:4}$ is associated with salinity or temperature lower than 10 °C in lacustrine environments (Blanz et al. 2005; Araie et al. 2018). Given that the isolation of the East Sea and surface freshening due to the lowered sea level during glacial periods, alkenone $C_{37:4}$ synthesis may be associated with much fresher environments of the East Sea. Unfortunately, supporting evidence such as haptophyte assemblage data are currently unavailable in the East Sea. Further studies should discern the effect of salinity and temperature lower than 10 °C on alkenone-based SST in the East Sea to interpret this proxy with confidence.

The most remarkable characteristics of the reconstructed SSTs can be summarized as follows. First, the unexpectedly higher SSTs (20.3 °C) during MIS 2 might have been driven by the enhanced inflow of the WTC (Ishiwatari et al. 1999), and possible surface freshening (Oba et al. 1991; Lee and Nam 2003). Second, the SST variation during MISs 10–12 was minor. To date, SSTs during MISs 10–12 have not been reported in sediments from the Korean Plateau in the East Sea, which does not seem to follow global SST trends. These small changes in SSTs during MIS10-12 are likely an important oceanographic characteristic of the Korea Plateau in the East Sea, which might be associated with local oceanographic changes with relatively shallow water depth. Therefore, the general assumption that global SSTs were similar worldwide during glacial periods cannot be applied to the Korea Plateau in the East Sea. Furthermore, our results show a relatively small decrease in SSTs although large fluctuation of SSTs were observed between glacial and interglacial periods. This further suggests that the SST variations observed in the study area reflect more local oceanographic conditions rather than global oceanic conditions.

5.3 Paleoceanographic Regime Shift on the Korea Plateau Over the Past 500 kyr

Paleoceanographic variations in the East Sea clearly associated with sea level changes, which were > 120 m during the LGM and exhibited repeated changes between glacial and interglacial periods (Oba et al. 1991; Tada et al. 1999). This result indicates that the East Sea was isolated physiographically, which would have led to freshwater input from the neighboring area (Oba et al. 1991; Lee and Nam 2003). Due to this freshwater influx, a relatively high-intensity negative shift in oxygen isotope values occurred during the LGM (Oba et al. 1991; Kim et al. 2000; Kido et al. 2007; Sagawa et al. 2018), which has been used as a stratigraphic criterion.

Based on the $\delta^{13}C_{org}$ and $\delta^{15}N_{org}$ ratios, paleoceanographic features such as paleoproductivity and circulation patterns may have undergone two modes on the Korea Plateau, differing from that modes that occurred in other parts of the East Sea. The first mode, consisting of strong negative coupling of the $\delta^{13}C_{org}$ and $\delta^{15}N_{org}$ ratios (SNCM), occurred in MISs 2, 10, and 12 (glacial periods). This mode is characterized by high C/N ratios, and low $\delta^{13}C_{org}$ and $\delta^{15}N_{org}$ ratios. The second mode (NODM) is characterized by relatively high $\delta^{13}C_{org}$ and $\delta^{15}N_{org}$ ratios and C/N ratio that did not exceed 12 (Figs. 4 and 5). However, the C/N ratio increased slightly during MIS 6 and 8. Although MIS 6 and 8 were glacial periods, they may represent an intermediate stage between SNCM to NODM. The higher TOC and carbonate contents and slight increase in the C/N ratios support this idea.

Assuming that the variations in $\delta^{15}N_{org}$ ratios were associated mainly with changes in nitrate utilization and productivity, these shifts in the ratio may reflect water column circulation changes around the Korea Plateau. When terrestrial inputs reached their maximum level at the peak of an SNCM period, i.e., MIS 2, 10 or 12, ocean conditions were unfavorable to high productivity. These SNCM periods are characterized by lower $\delta^{13}C_{org}$ and $\delta^{15}N_{org}$ excursion, suggesting enhanced terrestrial organic matter input. Previous studies have suggested that nitrogen isotope values may have decreased by about 3‰ below their initial values under anoxic conditions during the Holocene, whereas under oxic conditions, these values may have increased by 3‰ (Emmer and Thunell 2000). Another study suggested that alternating organic-rich dark layers and organic-poor light layers observed in deeper parts of the basins in the East Sea could be interpreted as reflecting changes in bottom-water oxygenation, which changed the paleo-circulation mode (Watanabe et al. 2007). This phenomenon can be attributed to terrestrial organic nitrogen input and denitrification caused by reduced ventilation during these periods. Lower $\delta^{15}N_{org}$ and $\delta^{13}C_{org}$ and high C/N ratios (Fig. 6) clearly support terrestrial input of organic matter.

This series of complicated oceanographic environmental changes appears to have occurred under alternating SNCM and NODM conditions with a transitional sub-mode (Fig. 7). During the glacial periods, intensified cold water formed at the northernmost part of the East Sea (Ikehara and Itaki 2007) may have affected the circulation over the Korea Plateau. However, relatively weak warm water may have been further weakened during this period, mostly due to the closure of the Korea Strait. A larger amount of terrestrial material was delivered to this site due to the intensified temperature gradient. However, the strong warm water came from the Korea Strait, and the relatively weak cold water domain modulated the oceanographic conditions of the Korea Plateau during the interglacial period. Even if the

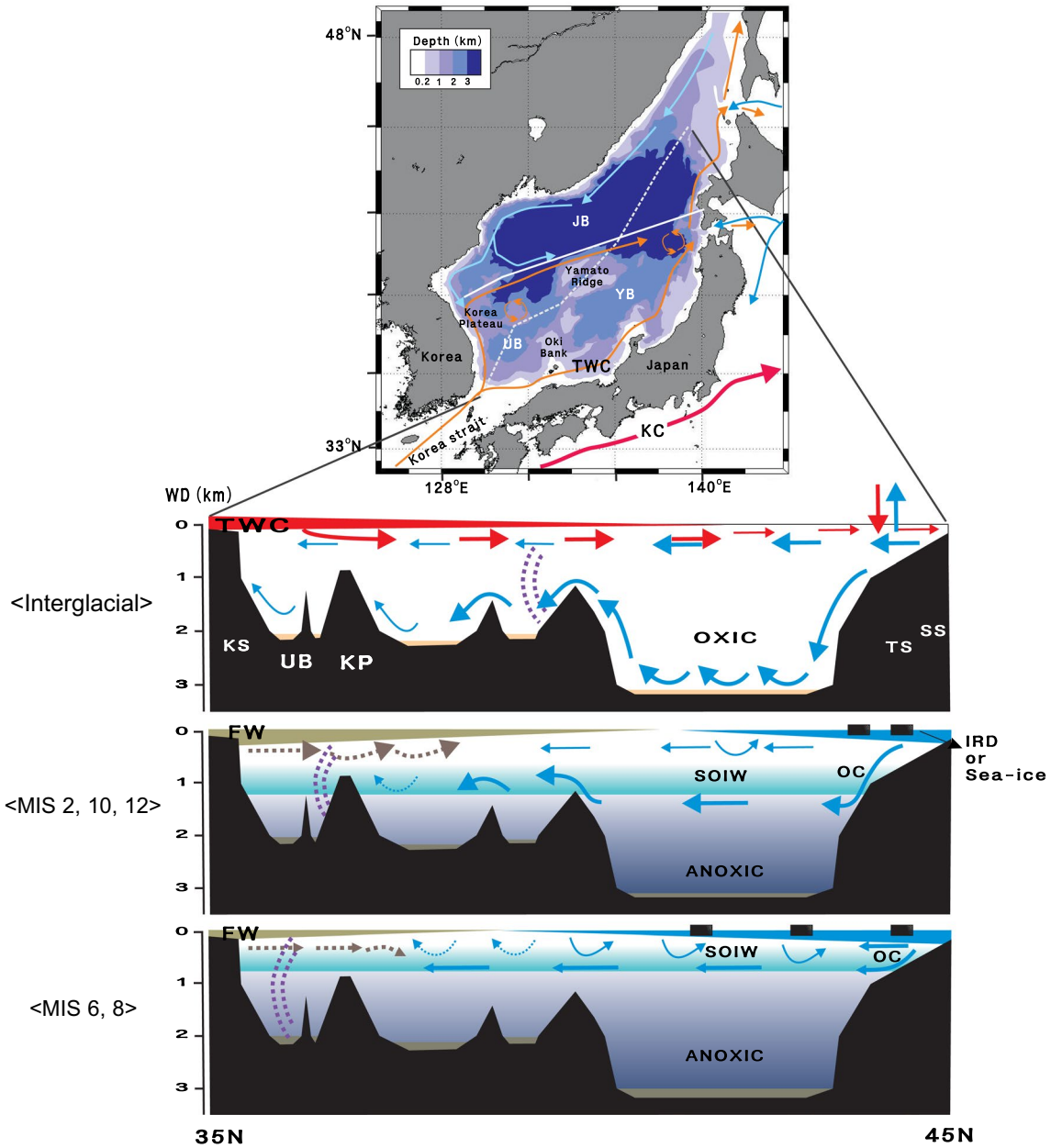

Fig. 7 Mode schematics for oceanographic conditions around the Korea Plateau, East Sea. Both modes were determined according to threshold conditions controlled by the high input of cold water (rectangular) from the north and warm water from the south, and by the intensity of intermediate water circulation. A sub-mode during MIS 6 and 8 is shown in the middle of the figure. Tan indicates freshwater intrusion during glacial periods and blue indicates the invasion of cold water from the north. *FW* Freshwater; *KC* Kuroshio Current; *OC* Oyashio Current; *SOIW* Suboxic Intermediate Water; *TWC* Tsushima Warm Current; *UB* Ulleung Basin. Broken lines during glacial periods indicate the position of subpolar fronts. These schematic modes were based on various references of Oba et al. (1991); Lee et al. (2003); Ikehara and Itaki (2007) etc.

rise and decline in amount of cold water and shutdown of the Korea Strait occurred during the glacial and interglacial periods, these changes may not have played important roles in determining the oceanographic conditions on the Korea Plateau. The degree of nitrogen utilization may have been influenced by two opposing environmental changes. The threshold condition may be reached in a short time, although this rapid shift should generally occur during transitional periods. Galbraith et al. (2004) described the use of nitrogen during glacial–interglacial periods. Likewise, biological productivity driven by nitrogen utilization at our site may have been associated with several complex factors such as the mixing rate of water masses.

The alternating sediment layers observed here could provide insight into our results. The low $\delta^{15}N_{org}$ values at the end of MIS 12, 10, and 2 may reflect an influx of terrestrial material and a degree of denitrification related to weak circulation changes. Although $\delta^{13}C_{org}$ increased at the boundary between MISs 8 and 7 and at the end of MIS 6, $\delta^{15}N_{org}$ values did not increase at these times. This finding indicates that the factors controlling the increasing trends of both $\delta^{13}C_{org}$ and $\delta^{15}N_{org}$ differed among MIS. This difference was probably caused by changes in ocean circulation on the Korea Plateau. These factors are closely associated with the influences of two different modes of water mass and sea-level conditions during glacial–interglacial periods.

6 Conclusions

Sedimentary lamination, excursions of high-resolution oxygen isotope values in foraminifera, and alkenone-based SST variations make it possible to reconstruct the refined stratigraphy of the Korean Plateau sediments in the East Sea. The age of the studied core covered the past 500 kyr, reaching the end of MIS 13, and recorded evidence of paleoceanographic regime shifts. The geochemical chronology established in this study revealed that the paleoceanographic conditions on the Korea Plateau may have differed from those in other parts of the East Sea, and these patterns were not uniform between glacial and interglacial periods or from one glacial period to another. The variations in $\delta^{13}C_{org}$ and $\delta^{15}N_{org}$ had two predominant modes over the last 500 kyr. The first was the SNCM, characterized by low $\delta^{13}C_{org}$ and $\delta^{15}N_{org}$, and was likely associated with the terrestrial organic matter influx and denitrification. These conditions occurred in MIS 2, 10, and 12. The second mode was NODM, with high TOC contents, characterized by high productivity and intermediate transitional conditions between glacial to interglacial periods. Therefore, the typical pattern of glacial–interglacial paleoceanographic phenomena observed in major basins of East Sea sediment are not applicable to the Korea Plateau. The most plausible causes of such difference are associated with eustatic sea-level changes during glacial-interglacial periods and with the location and water depths of the Korea Plateau, which is situated at the confluence of two currents, where topographic highs modulate oceanic conditions.

Acknowledgements This study was conducted as a part of a project titled "International Ocean Discovery Program" of K-IODP (PM62120) funded by the Ministry of Ocean and Fisheries, and also supported by the KIOST programs (PE99775). The first author thanks to Dr. Kido for providing original oxygen isotope data for the stratigraphic comparison and also thanks to anonymous reviewers for enhance the quality of manuscript.

Author Contributions SH: data curation, writing an original manuscript. J-KK: analysis, and figure drawing, editing. JK: writing and review. GYK: project administration, reviewing.

Data Availability We state that all the data in this study have not been published yet. We can upload these data in this paper and agree to archive them in appropriate repository as required.

References

Altabet MA, Francois R (1994) Sedimentary nitrogen isotopic ratio as a recorder for surface ocean nitrate utilization. Global Biogeochem Cycles 8:103–116. https://doi.org/10.1029/93GB03396

Ao H, Rohling EJ, Stringer C, Roberts AP, Dekkers M, Dupont-Nivet G, Yu J, Liu Q, Zhang P, Liu Z, Ma X, Zhou W, Jin Z, Xiao G, Wang H, Sun Q, Yang P, Peng X, Shi Z, Qiang X, An Z (2020) Two-stage mid-Brunhes climate transition and mid-Pleistocene human diversification. Earth Sci Rev 210:103354. https://doi.org/10.1016/j.earscirev.2020.103354

Araie H, Nakamura H, Toney JL, Haig HA, Plancq J, Shiratori T, Leavitt PR, Seki O, Ishida K-I, Sawada K, Suzuki I, Shiraiwa Y (2018) Novel alkenone-producing strains of genus *Isochrysis* (Haptophyta) isolated from Canadian saline lakes show temperature sensitivity of alkenones and alkenoates. Org Geochem 121:89–103. https://doi.org/10.1016/j.orggeochem.2018.04.008

Bahk JJ, Chough SK, Han SJ (2000) Origins and paleoceanographic significance of laminated muds from the Ulleung Basin, East Sea (Sea of Japan). Mar Geol 162:459–477. https://doi.org/10.1016/S0025-3227(99)00079-1

Bahk JJ, Lee KE, Chough SK (2005) Relative role of productivity vs. stagnation in dark laminated mud formation during the last 25,000 years in the Ulleung Basin, East/Japan Sea. Geosci J 9:297–304

Bendle J, Rosell-Mele A, Ziveri P (2005) Variability of unusual distributions of alkenones in the surface waters of the Nordic Sea. Paleoceanography 20:PA2001. https://doi.org/10.1029/2004PA001025

Blanz T, Emeis K-C, Siegel H (2005) Controls on alkenone unsaturation ratios along the salinity gradient between the open ocean and the Baltic Sea. Geochim Cosmochim Acta 69:3589–3600. https://doi.org/10.1016/j.gca.2005.02.026

Brassell SC, Eglinton G, Marlowe IT, Pflaumann U, Sarnthein M (1986) Molecular stratigraphy: a new tool for climatic assessment. Nature 320:129–133. https://doi.org/10.1038/320129a0

Burckle LH, Brunner CA, Alexandrovich J, DeMenocal P, Briscoe J, Hamano Y, Heusser L, Ingle JC, Kheradyar T, Koizumi I, Krusiek KAO, Ling H-Y, Muza JP, Rahamn A, Sturz A, Vigliotti L, White LD, Wippern JJM, Yamanoi T (1992) Biostratigraphic and biochronologic synthesis of Legs 127 and 128: Sea of Japan. In: Tamaki K, Suyehiro K, Allan J, McWilliams E (eds) Proceedingsof the Ocean Drilling Program Scientific Results: 127/128. Part 2, Ocean Drilling Program, College Station, pp 1197–1218

Calvert SE, Nielsen B, Fontugne MR (1992) Evidence from nitrogen isotope ratios for enhanced productivity during formation for eastern Mediterranean sapropels. Nature 359:223–225. https://doi.org/10.1038/359223a0

Charvet J, Grimm K, Griffin J, Jolivet L, Pouclet A, Panis D (1992) Structureal features in Leg 128 cores: Relationship with the tectonic evolution of the Japan Sea. In: Tamaki K, Suyehiro K, Allan J, McWilliams E (eds) Proceedings of the Ocean Drilling Program Scientific Results: 127/128. Part 2, Ocean Drilling Program, College Station, pp 1175–1193

Dansgaard W, Johnsen SJ, Clausen HB, Dahl-Jensen D, Gundestrup NS, Hammer CU, Hvidberg CS, Steffensen JP, Sveinbjornsdottir AE, Jouzel J, Bond G (1993) Evidence for general instability of

past climate from a 250-kyr ice-core record. Nature 364:218–220. https://doi.org/10.1038/364218a0

Emmer E, Thunell RC (2000) Nitrogen isotope variation in Santa Barbara Basin sediments: implications for denitrification in the eastern tropical North Pacific during the last 50,000 years. Paleoceaography 15:377–387. https://doi.org/10.1029/1999PA000417

Fairbanks RG (1989) A 17,000-year glacio-eustatic sea-level record: influences of glacial melting rates on the Younger Dryas events and deep-ocean circulation. Nature 342:637–642

Farrell JW, Prell WL (1989) Climate change and $CaCO_3$ preservation: an 800,000 year bathymetric reconstruction from the central quatorial Pacific Ocean. Paleoceanography 4:447–466. https://doi.org/10.1029/PA004i004p00447

Feely RA, Sabine CL, Lee K, Berelson W, Kleypas J, Fabry VJ, Millero FJ (2008) Impact of anthropogenic CO_2 on the $CaCO_3$ system in the oceans. Science 305:362–366. https://doi.org/10.1126/science.1097329

Freudenthal T, Wagner T, Wenzhofer F, Zabel M, Wefer G (2001) Early diagenisis of organic matter from sediments of the eastern subtropical Atlantic: evidence from stable nitrogen and carbon isotopes. Geochim Cosmochim Acta 65:1795–1808. https://doi.org/10.1016/S0016-7037(01)00554-3

Galbraith ED, Kienast M, Pedersen T, Calvert SE (2004) Glacial-interglacial modulation of the marine nitrogen cycle by high-latitude O_2 supply to the global thermocline. Paleoceanography 19:PA4007. https://doi.org/10.1029/2003PA001000

Ganeshram RS, Pedersen TF, Calvert SE, McNeill GW, Fontugne MR (2000) Glacial-interglacial variability in denitrification in the world's oceans: cause and consequences. Paleoceanography 15:361–376. https://doi.org/10.1029/1999PA000422

Harada N, Shin KH, Murata A, Uchida M, Nakatani T (2003) Characteristics of alkenones synthesized by a bloom of *Emiliania huxleyi* in the Bering Sea. Geochim Cosmochim Acta 67:1507–1519. https://doi.org/10.1016/S0016-7037(02)01318-2

Harada N, Sato M, Sakamoto T (2008) Freshwater impacts recorded in tetraunsaturated alkenones and alkenon sea surface temperatures from the Okhotsk Sea across millennial-scale cycles. Paleoceanography. https://doi.org/10.1029/2006PA001410

Hyun S, Bahk JJ, Suk BC, Park BK (2007) Alternative modes of Quaternary pelagic biosiliceous and carbonate sedimentation: a perspective from the East Sea (Japan Sea). Paleogeogr Paleoclimatol Paleoecol 247:88–99. https://doi.org/10.1016/j.palaeo.2006.11.023

Hyun S, Kim CH, Jou HT, Kim JK, Park CH (2010) Characteristics of surface sediments distribution and submarine topography around Dokdo Island, Korea. J Geol Soc Korea 46:647–660

Hyun S, Kim JM, Yim UH, Shim WJ, Yoon SH, Woo KS (2013) Variations in sea surface temperature based on alkenones in Korea Plateau sediments of the East Sea (Sea of Japan) over the last 300,000 year. J Asian Earth Sci 66:140–149. https://doi.org/10.1016/j.jseaes.2012.12.036

Ikehara K, Itaki T (2007) Millennial-scale fluctuations in seasonal sea-ice and deep-water formation in the Japan Sea during the late Quaternary. Paleogeogr Paleoclimatol Paleoecol 247:131–143. https://doi.org/10.1016/j.palaeo.2006.11.026

Ingle JC (1992) Subsidence of the Japan Sea: Stratigraphic evidence from ODP Sites and onshore sections. In: Tamaki K, Suyehiro K, Allan J, McWilliams E (eds) Proceedings of the Ocean Drilling Program Scientific Results: 127/128. Part 2, Ocean Drilling Program, College Station, pp 1197–1218

Irino T, Tada R (2002) High resolution reconstruction of variation in Aeolian dust (Kosa) deposition at ODP site 797, the Japan Sea, during the last 200 ky. Global Planetary Change 35:107–120

Irino T, Tada R, Ikehara K, Sagawa T, Karasuda A, Kurokawa S, Seki A, Lu S (2018) Construction of perfectly continuous records of physical properties for dark-light sediment sequences collected from the Japan Sea during Integrated Ocean Drilling Program Expedition 346 and their potential utilities as paleocanographic studies. Prog Earth Planet Sci 5:23. https://doi.org/10.1186/s40645-018-0176-7

Ishiwatari R, Yamada K, Matsumoto K, Hoitatsu M, Naraoka H (1999) Organic molecular and carbon isotope records of the Japan Sea over the past 30 kyr. Paleoceanography 14:260–270. https://doi.org/10.1029/1998PA900014

Kaiser J, Wang KJ, Rott D, Li G, Zheng Y, Amaral-Zettler L, Arz HW, Huang Y (2019) Changes in long chain alkenone distribution and isochrysidales groups along the Baltic Sea salinity gradient. Organic Geocheomistry 127:92–103. https://doi.org/10.1016/j.orggeochem.2018.11.012

Keigwin WD, Gorbarenko SA (1992) Sea level, surface salinity of the Japan Sea, and the Younger Dryas event in the northwest Pacific Ocean. Quatern Res 37:346–360. https://doi.org/10.1016/0033-5894(92)90072-Q

Khim BK, Ikehara K, Bahk JJ, Irino T (2008) Increased negative anomalies of sedimentary organic matter $\delta^{13}C$ and $\delta^{15}N$ values in the East Sea (Sea of Japan) during the full glaciation of the late Quaternary. Quatern Int 176–177:25–35. https://doi.org/10.1016/j.quaint.2007.05.016

Khim BK, Tada R, Park YH, Bahk JJ, Kido Y, Itaki T, Ikehara K (2009) Correlation of TL layers for the synchronous paleoceanographic events in the East Sea (Sea of Japan) during the late Quaternary. Geosci J 13:113–120

Kido Y, Minami I, Tada R, Fujine K, Irino T, Ikehara K, Chun JH (2007) Orbital-scale stratigraphy and high-resolution analysis of biogenic components and deep-water oxygenation conditions in the Japan Sea during the last 640 kyr. Paleogeogr Paleoclimatol Paleoecol 247:32–49. https://doi.org/10.1016/j.palaeo.2006.11.020

Kienast SS, Calvert SE, Pedersen F (2002) Nitrogen isotope and productivity variations along the northeast Pacific margin over the last 120 kyr: surface and subsurface paleoceanography. Paleoceanography 17:1055. https://doi.org/10.1029/2001PA000650

Kim JM, Kennett JP, Park BK, Kim DC, Kim GY, Roark EB (2000) Paleoceanographic changes during the last deglaciation, East Sea of Korea. Paleoceanography 15:254–266. https://doi.org/10.1029/1999PA000393

Kim T-W, Lee K, Feely RA, Sabine CL, Chen C-TA, Jeong HJ, Kim KY (2010) Prediction of Sea of Japan (East Sea) acidification over the past 40 years using a multiparameter regression model. Global Biogeochem Cycle 24:GB3005. https://doi.org/10.1029/2009GB003637

Lamb AL, Wilson GP, Leng MJ (2006) A review of coastal paleoclimate and relative sea-level reconstructions using ^{13}C and C/N ratios in organic material. Earth Sci Rev 75:29–57. https://doi.org/10.1016/j.earscirev.2005.10.003

Lee KE (2007) Surface water changes recorded in Late Quaternary marine sediments of the Ulleung Basin, East Sea (Japan Sea). Paleogeogr Paleoclimatol Paleoecol 247:18–31. https://doi.org/10.1016/j.palaeo.2006.11.019

Lee E, Nam S (2003) Freshwater supply by Korean rivers to the East Sea during the last glacial maximum: a review and new evidence from the Korea Strait region. Geo-Mar Letter 23:1–6. https://doi.org/10.1007/s00367-003-0118-1

Lee SH, Chough SK, Back GG, Kim YB, Sung BS (1999) Gradual downslope change in high-resolution acoustic characters and geometry of large-scale submarine debris lobes in Ulleung Basin, East Sea (Sea of Japan), Korea. Geo-Mar Letter 19:254–261. https://doi.org/10.1007/s003670050116

Lee KE, Bahk JJ, Choi J (2008) Alkenone temperature estimates for the East Sea during the last 190,000 years. Org Geochem 39:741–753. https://doi.org/10.1016/j.orggeochem.2008.02.003

Lehmann MF, Bernasconi SM, Barbieri A, Mckenzin JA (2002) Preservation of organic matter and alternation of its carbon and nitrogen

isotope composition during simulated and in situ early sedimentary diagenesis. Geochimica Cosmochimca Acta 66:3573–3584. https://doi.org/10.1016/S0016-7037(02)00968-7

Lim J, Fujiki T (2011) Vegetation and climate variability in East Asia driven by low latitude ocean forcing during the middle to late Holocene. Quatern Sci Rev 30:2487–2497. https://doi.org/10.1016/j.quascirev.2011.05.013

Lisiecki LE, Raymo ME (2005) A Pliocene-Pleistocene stack of 57 globally distributed benthic $\delta^{18}O$ records. Paleoceanography 20:PA1103. https://doi.org/10.1029/2004PA001071

Martinson DC, Pisias NG, Hays JD, Imbrie J, Moore TCJ, Shackleton NJ (1987) Age dating and the orbital theory of the ice ages: development of a high-resolution 0 to 300000-year chronostratigraphy. Quatern Res 27:1–29. https://doi.org/10.1016/0033-5894(87)90046-9

Mobius J, Gaye B, Lahajnar N, Bahlmann E, Emeis KC (2011) Influence of diagenesis on sedimentary $\delta^{15}N$ in the Arabian Sea over the last 130 kyr. Mar Geol 284:127–138

Nagashima K, Tada R, Tani A, Sun Y, Isozaki Y, Toyoda S, Hasegawa H (2011) Millennial-scale oscillations of the westerly jet path during the last glacial period. J Asian Earth Sci 40:1214–1220. https://doi.org/10.1016/j.jseaes.2010.08.010

Nagel B, Gaye B, Kodina LA, Lahajnar N (2009) Stable carbon and nitrogen isotopes as indicators for organic matter sources in the Kara Sea. Mar Geol 266:42–51. https://doi.org/10.1016/j.margeo.2009.07.010

Naidu AS, Cooper LW, Finney BP, Macdonald RW, Alexander C, Semiletov IP (2000) Organic carbon isotope ratio ($\delta^{13}C$) of Arctic Amerasian continental shelf sediments. Int J Earth Science 89:522–532. https://doi.org/10.1007/s005310000121

Nakatsuka T, Handa E, Wada E, Wong CS (1992) The dynamic changes of stable isotopic ratios of carbon and nitrogen in suspended and sediment particulate organic matter during a phytoplankton bloom. J Mar Res 50:267–296

Nakatsuka T, Watanabe K, Handa N, Matsumoto WE (1995) Glacial to interglacial surface nutrient variations of Bering deep basins recorded by ^{13}C and ^{15}N of sedimentary organic matter. Paleoceanography 10:1047–1061. https://doi.org/10.1029/95PA02644

Nitani H (1972) Beginning of the Kuroshio. In: Stommel H, Yoshida K (eds) Kuroshio, its physical aspects. Univ. Tokyo Press, Tokyo, pp 129–163

Oba T, Pedersen TF (1999) Paleoclimatic significance of eolian carbonate supplied to the Japan Sea during the last glacial maximum. Paleoceagnography 14:34–41. https://doi.org/10.1029/98PA02507

Oba T, Kato M, Kitazoto H, Koizumi I, Omura A, Sakao T, Takayama T (1991) Paleoenvironmental changes in Japan Sea during the last 85,000 years. Paleoceanography 6:499–518. https://doi.org/10.1029/91PA00560

Prahl FG, Wakeham SG (1987) Calibration of unsaturation patterns in long-chain ketone compositions for paleotemperature assessment. Nature 330:367–369. https://doi.org/10.1038/330367a0

Prahl FG, Muehlhausen LA, Zahnle DL (1988) Further evaluation of long-chain alkenones as indicators of paleoceanographic conditions. Geochim Cosmochim Acta 52:2303–2310. https://doi.org/10.1016/0016-7037(88)90132-9

Sagawa T, Nagahashi Y, Satoguchi Y, Holbourn A, Itaki T, Gallagher SJ, Saavedra-Pellitero M, Ikehara K, Irono T, Tada R (2018) Integrated tephrostratigraphy and stable isotope stratigraphy in the Japan Sea and East China Sea using IODP Sites U1426, U1427, and U1429, Expedition 346 Asian monsoon. Prog Earth Planet Sci 5:18. https://doi.org/10.1186/s40645-018-0168-7

Sawada K, Handa N (1998) Variability of the path of the Kuroshio ocean current over the past 25,000 years. Nature 392:592–595. https://doi.org/10.1038/33391

Seki A, Tada R, Kurokawa S, Murayama M (2019) High-resolution Quaternary record of marine organic carbon content in the hemipelagic sediments of the Japan Sea from bromine counts measured by XRF core scanner. Prog Earth Planet Sci 6:1. https://doi.org/10.1186/s40645-018-0244-z

Shen X, Wan S, France-Laord C, Clift PD, Tada R, Revillon S, Shi X, Zhao D, Liu Y, Yin X, Song Z, Li A (2017) History of Asian eolian input to the Sea of Japan since 15 Ma: links to Tibetan uplift or global cooling? Earth Planet Sci Lett 424:296–308. https://doi.org/10.1016/j.epsl.2017.06.053

Stein R (1990) Organic carbon/sedimentation rate relationship and its paleoenvironmental significance for marine sediments. Geo-Mar Letter 10:37–44. https://doi.org/10.1007/BF02431020

Stuiver M, Reimer PJ (1993) Extended 14C database and revised CALIB radiocarbon calibration program. Radiocarbon 35:215–230. https://doi.org/10.1017/S0033822200013904

Suh YJ, Hyun S, Park C (2013) Late Quaternary paleoceanographic changes in the northeastern Ulleung Basin, East Sea, inferred from variations in biogenic components. Ocean Sci J 48:289–300. https://doi.org/10.1007/s12601-013-0027-9

Tada R, Iijima A (1992) Lithostratigraphy and compositional variation of Neogene hemipelagic sediments in the Japan Sea. In: Tamaki K, Suyehiro K, Allan J, McWilliams E (eds) Proceedings of the Ocean Drilling Program Scientific Results: 127/128. Part 2, Ocean Drilling Program, College Station, pp 1197–1218

Tada R, Irino T, Koizumi I (1999) Land-ocean linkages over orbital and millennial timescale recorded in late Quaternary sediments of the Japan Sea. Paleoceanography 14:236–247. https://doi.org/10.1029/1998PA900016

Tada R, Irino T, Ikehara K, Karasuda A, Sugisaki S, Xuan C, Sagawa T, Itaki T, Kubota Y, Lu S, Seki A, Murry RW, Alvarez-Zarikian C, Anderson WT, Bassetti M-A, Brace BJ, Clemens SC, Costa Gurgel M, Dickens GR, Dunlea AG, Gallagher SJ, Giosan L, Henderson ACG, Holbourn AE, Kinsley CW, Lee GS, Lee KE, Lofi J, Lopes CICD, Saavedra-Pellitero M, Peterson LC, Singh RK, Toucanne S, Wan S, Zheng H, Ziegler M (2018) High-resolution and high-precision correlation of dark and light layers in the Quaternary hemipelagic sediments of the Japan Sea recovered during IODP Expedition 346. Prog Earth Planet Sci 5:19. https://doi.org/10.1186/s40645-018-0167-8

Tyson RV (1995) Sedimentary organic matter: organic facies and palynofacies. Chapman ad Hall, London, p 615

Ujiie H, Ichikura M (1973) Holocene to uppermost Pleistocene planktonic foraminiferas in a piston core from off San'in district, Sea of Japan. Trans Proc Paleontol Soci Jpn 91:137–150

Wang KJ, Huang Y, Majaneva M, Belt ST, Liao S, Novak J, Kartzinel TR, Herbert TD, Richter N, Cabedo-Sanz P (2021) Group 2i Isochrysidales produce characteristic alkenones reflecting sea ice distribution. Nature comm 12:15. https://doi.org/10.1038/s41467-020-20187-z

Watanabe S, Tada R, Ikehara K, Fujine K, Kido Y (2007) Sediment fabrics, oxygenation history, and circulation modes of Japan Sea during the late Quaternary. Paleogeogr Paleoclimatol Paleoecol 247:50–64

Yokoyama Y, Naruse T, Ogawa NO, Tada R, Kitazato H, Ohkouchi N (2006) Dust influx reconstruction during the last 26,000 years inferred from a sedimentary leaf wax record from the Japan Sea. Glob Planet Change 54:239–250. https://doi.org/10.1016/j.gloplacha.2006.06.022

Yoon JH, Kawamura H (2002) The formation and circulation of the intermediate water in the Japan Sea. J Oceanogr 58:197–211. https://doi.org/10.1023/A:1015893104998

Zhai L, Wan S, Colin C, Zhao D, Ye Y, Song Z, Yin X, Shi X, Li A (2021) Deep-Water formation in the North Pacific during the Late Miocene global cooling. Paleoceanogr Paleoclimatol 36:e2020PA003946. https://doi.org/10.1029/2020PA003946